

point, we assume an interlayer mechanism: For any mechanism involving coupling pairs within the planes, the entire condensation energy does not depend crucially on  $\varphi$ . The current is  $2e$  times the derivative of this energy with phase; hence, the superconducting binding energy is given by

$$F_{\text{cond}} = \frac{\hbar J_J}{e} \cos \varphi \quad (5)$$

(accounting for interactions with two neighboring layers). The "Josephson" plasma frequency (7), which in this case is the plasma frequency itself, is given by

$$(\hbar \omega_J)^2 = \frac{\hbar J_J 2e^2}{e \epsilon c} = \frac{2e\hbar}{\epsilon d} J_J \quad (6)$$

( $\epsilon$  is  $\sim 20$ , and  $d$  is the  $c$ -axis lattice constant). From the value  $50 \text{ cm}^{-1}$  for  $\omega_J$ ,  $\hbar J_J / 2e \approx 4/3 \text{ K}$ . This is then equated to the value of  $F_{\text{cond}}$  per unit cell. In any reasonable theory, and in fact in that of Chakravarty and Anderson (8)

$$F_{\text{cond}} \approx \frac{1}{2} N(0) \Delta^2 \quad (7)$$

simply by energy-entropy balance. With a density of states at  $\omega = 0$  of  $N(0) \approx 1/t_{\parallel} \approx (1 \text{ eV})^{-1}$  (where  $t_{\parallel}$  is the in-plane element of the kinetic energy matrix  $t$ ), this gives

$$\Delta \approx 100 \text{ K} \quad (8)$$

which is correct to within a factor 2. That is, the Josephson and condensation energies are the same, at least within the factor 2 accuracy of these estimates.

The anisotropy of the penetration depth will, in these materials, be greater than expected according to band theory and will give too large a value of the band mass relative to band calculations. The constant corresponding to  $n/m$  in the expression

$$\frac{1}{\lambda^2} = \frac{4\pi n e^2}{m c^2} \quad (9)$$

which is proportional to  $t_{\perp}^2/t_{\parallel}$  in conventional theory ( $t_{\perp}$  is the out-of-plane element), will be more like  $t_{\perp}^4/t_{\parallel}^3$ . Here I have observed that both the coherence length  $\xi$  and the penetration depth  $\lambda$ , the two parameters of Ginsberg-Landau theory, are uniquely determined in the  $c$  direction by the assumption of interlayer coupling as the mechanism for  $T_c$  if the material has only one type of layer. The coherence length (from the assumption in Eq. 5) is simply  $d$  (actually  $d/\sqrt{2}$  or  $\sim 4 \text{ \AA}$ ), and the penetration depth  $c/\omega_J$  is determined from Eq. 6 [ $\sim 2 \times 10^{-2} \text{ cm}$ , in  $(\text{LaSr})_2\text{CuO}_4$ ]. The coherence length is in fair agreement with direct experiments (9).

I can see no alternative explanation of these very striking experimental data.

Other single-layer materials, especially the Tl and Hg compounds, should be studied in the same way. Multilayers such as YBCO (yttrium barium copper oxide) will have much more complex infrared spectra, which nonetheless would be of interest to probe carefully. In these cases, there should be two Josephson-type frequencies, corresponding to the two different interlayer matrix elements  $t_{\perp>}^2$  and  $t_{\perp<}^2$ , with the smaller one corresponding to the penetration depth and coherence length (because phase stiffness adds by inverses) and the larger one to  $T_c$  or  $\Delta$ , because  $T_c$  adds directly [evidence of such a second frequency is suggested in some experiments (2)]. By this reasoning, the coherence length should satisfy

$$\xi \approx \frac{d t_{\perp<}^2}{(t_{\perp>}^2 + t_{\perp<}^2)} \quad (10)$$

where  $t_{\perp<}^2$  and  $t_{\perp>}^2$  are, respectively, the larger and the smaller of the interlayer tunneling coupling constants. This result is in accord with the existing observations. Multilayers will have a corresponding increase in  $\lambda_c$  (penetration depth for current parallel to the  $c$  direction) as well.

## REFERENCES AND NOTES

1. K. Tanasaka, Y. Nakamura, S. Uchida, *Phys. Rev. Lett.* **69**, 1455 (1992).
2. T. Timusk, personal communication.
3. J. H. Kim *et al.*, in preparation.
4. K. Tamasaku, T. Ito, H. Takagi, S. Uchida, *Phys. Rev. Lett.* **72**, 3088 (1994).
5. J. M. Wheatley, T. C. Hsu, P. W. Anderson, *Nature* **333**, 121 (1988); P. W. Anderson *et al.*, *Physica C* **153-155**, 527 (1988); P. W. Anderson, in *Strong Correlation and Superconductivity*, H. Fukuyama, S. Maekawa, A. P. Malozemoff, Eds. (Springer-Verlag, Berlin, 1989), p. 2; \_\_\_\_\_ and Y. Ren, in *High Temperature Superconductivity Proceedings*, K. Bedell *et al.*, Eds. (Addison-Wesley, Reading, MA, 1990), pp. 3-33.
6. D. G. Clarke, S. P. Strong, P. W. Anderson, *Phys. Rev. Lett.* **72**, 3218 (1994).
7. P. W. Anderson, *Weak Superconductivity: The Josephson Tunneling Effect* (5th International School of Physics, Ravella, Italy, 1963), E. R. Caianello, Ed. (Academic Press, New York, 1964), vol. 2, p. 113. The term "Josephson plasma frequency" was first mentioned in this paper.
8. S. Chakravarty and P. W. Anderson, *Phys. Rev. Lett.* **72**, 3859 (1994).
9. M. Suzuki and M. Hikita, *Phys. Rev. B* **44**, 249 (1991).
10. I acknowledge communication of results by T. Timusk, as well as a discussion, and particularly extensive discussions with D. Van der Marel and T. M. Rice. I also was stimulated by queries from R. Laughlin. This work was supported by NSF grants DMR-9104873 and DMR-9224077.

21 October 1994; accepted 10 March 1995

## Water on the Sun

Lloyd Wallace, Peter Bernath,\* William Livingston, Kenneth Hinkle, Jennifer Busler, Bujin Guo, Keqing Zhang

High-resolution infrared spectra of sunspot umbrae have been recorded with the 1-meter Fourier transform spectrometer on Kitt Peak. The spectra contain a very large number of water absorption features originating on the sun. These lines have been assigned to the pure rotation and the vibration-rotation transitions of hot water by comparison with high-temperature laboratory emission spectra.

The hot water molecule is the most important source of infrared opacity in the spectra of oxygen-rich late-type stars (1). Water is particularly prominent in the spectra of variable red giant stars (Mira variables) (2) and in other cool M-type stars (3). For very cool stars ("brown dwarfs"), water is predicted to be the most abundant molecule after hydrogen (1, 4).

L. Wallace and K. Hinkle, Kitt Peak National Observatory, National Optical Astronomy Observatories, Post Office Box 26732, Tucson, AZ 85726, USA.

P. Bernath, Department of Chemistry, University of Waterloo, Waterloo, Ontario, Canada N2L 3G1, and Department of Chemistry, University of Arizona, Tucson, AZ 85721, USA.

W. Livingston, National Solar Observatory, National Optical Astronomy Observatories, Post Office Box 26732, Tucson, AZ 85726, USA.

J. Busler, B. Guo, K. Zhang, Department of Chemistry, University of Waterloo, Waterloo, Ontario, Canada N2L 3G1.

\*To whom correspondence should be addressed.

The water molecule was discovered in molecular clouds in 1969 on the basis of the maser transition from  $6_{16}$  to  $5_{23}$  at 22 GHz (5). In spite of the large rotational constants, which place most transitions in the submillimeter region, many masing transitions are known for numerous objects (6). The water masers are thought to be collisionally pumped, and they are often associated with star-forming regions (6).

Because water is a strong absorber in Earth's atmosphere, there is a severe problem in detecting cool extraterrestrial water from the ground. Fortunately, the pure rotation and the vibration-rotation lines of hot water can pass through Earth's atmosphere because the large rotational constants of water ( $A_0 = 27.877 \text{ cm}^{-1}$ ,  $B_0 = 14.512 \text{ cm}^{-1}$ , and  $C_0 = 9.289 \text{ cm}^{-1}$ ) shift the highly excited transitions well away from the telluric absorptions of cooler water.

At 5785 K (7), the photosphere of our sun is too hot to permit water to exist, although the hydroxyl (OH) free radical is well known (8, 9). It has been calculated that at a temperature of about 3900 K the concentrations of water and OH are equal; below this temperature, water is the dominant oxygen-containing molecule (4) as well as the dominant opacity source.

Sunspots appear dark against the solar disk because they are cooler than its photosphere (Fig. 1) (7). We have recorded and reduced the infrared (IR) spectra of two sunspot umbrae; one spectrum covers the region from 1.16 to 5.1  $\mu\text{m}$  (1970 to 8640  $\text{cm}^{-1}$ ) and the other the region from 8.1 to 21  $\mu\text{m}$  (470 to 1233  $\text{cm}^{-1}$ ). The first spectrum includes the 1.25-, 2.2-, 3.4-, and 5- $\mu\text{m}$  atmospheric windows (called the J, K, L, and M bands, respectively) and the second covers the 10- $\mu\text{m}$  (N band) window through Earth's atmosphere. These spectra contain numerous atomic and molecular absorption features arising from CO, OH, HCl, HF, CN, SiO, and H<sub>2</sub>O. All of these molecules have been reported before except water (8). W. S. Benedict made some identifications of H<sub>2</sub>O in the near-IR (1.1 to 2.5  $\mu\text{m}$ ) in Hall's 1970 sunspot atlas (10), but the work was never completed and is unpublished. We report here on the identification of numerous water lines in sunspots.

The spectra in the region from 1970 to 8640  $\text{cm}^{-1}$  were obtained on the morning of 26 July 1991 with the 1-m Fourier transform spectrometer (FTS) at the McMath-Pierce telescope of the National Solar Observatory on Kitt Peak (11). A 7-arc sec

FTS entrance aperture was positioned on the darkest part of the mature sunspot umbra (diameter, 29 arc sec) (Fig. 1). The lower wave number limit was set by the InSb detector and the upper limit by a silicon filter. Spectra were recorded at air masses of 1.5 and 2.3 with a resolution of 0.015  $\text{cm}^{-1}$ . By definition, when the telescope points at the zenith, the radiation from an object passes through 1 air mass.

We used the two spectra at different air masses to correct for atmospheric absorption by extrapolating to zero air mass. This point-by-point extrapolation is possible with high signal-to-noise spectra but, of course, fails in the centers of strong absorption features. The final spectra were smoothed with a binomial filter of 0.024  $\text{cm}^{-1}$  full width at half maximum (FWHM) from 1970 to 8000  $\text{cm}^{-1}$  and 0.037  $\text{cm}^{-1}$  FWHM for 8000 to 8640  $\text{cm}^{-1}$ .

A magnetic field strength of 0.336 T (3360 G) was determined from the Zeeman splitting of a Ti atomic line at 4481  $\text{cm}^{-1}$ . The Zeeman effect typically broadens or splits atomic lines to 0.7  $\text{cm}^{-1}$  (FWHM) for a magnetic field of 3000 G at 4100  $\text{cm}^{-1}$  for a Landé  $g$  value of 2.5. Molecular lines have smaller widths of 0.07  $\text{cm}^{-1}$  (near 4100  $\text{cm}^{-1}$ ) determined by mass motion (thermal and turbulent Doppler broadening). The effective temperature of the sunspot is about 3300 K as determined by the strength of the 2-0 CO vibrational band head at 4360  $\text{cm}^{-1}$  (12). The effective spectral class of the umbra of the sunspot is M2 to M5 on this basis.

A typical page from the spectral atlas

produced for this sunspot (11) is shown in Fig. 2. There is a broad Si I line at 2704.10  $\text{cm}^{-1}$ , a quartet of strong OH vibration-rotation lines at 2702 to 2706  $\text{cm}^{-1}$  (9), the P(8) line of the 1-0 vibration-rotation band of H<sup>35</sup>Cl at 2703.01  $\text{cm}^{-1}$  (13, 14), and a few scattered H<sub>2</sub>O lines that can be identified (for example, 2710.19  $\text{cm}^{-1}$  is the 22<sub>13,10</sub> to 21<sub>12,9</sub> rotational line of the 001 to 010 vibrational band) with the currently available H<sub>2</sub>O energy levels (15). Ultimately, lines from 10 vibration-rotation bands were identified (11).

Although H<sub>2</sub>O has been studied extensively both experimentally (15-17) and theoretically (18), the reported energy levels are inadequate to identify all of the lines in the umbral spectra. There are numerous additional strong and weak lines (Fig. 2) that undoubtedly belong to water but cannot yet be assigned.

The 10- $\mu\text{m}$  spectrum (470 to 1233  $\text{cm}^{-1}$ ) of a different umbra (19) shows an even denser set of absorption lines (Fig. 3B). This spectrum was recorded for other purposes on 4 March 1982 by R. Noyes, J. Brault, R. Hubbard, and J. Wagner. A KCl beam splitter was used, and the spectrometer resolution was 0.005  $\text{cm}^{-1}$ . The "seeing" was very good, and the sunspot showed deep and dense molecular absorption. A reference spectrum of the penumbra of the spot was also recorded, and we used it to correct for telluric absorption by dividing the umbral spectrum by the scaled reference spectrum. Figure 3A presents the reference spectrum (top trace) and the umbral spectrum (lower trace), whereas in Fig. 3B there are

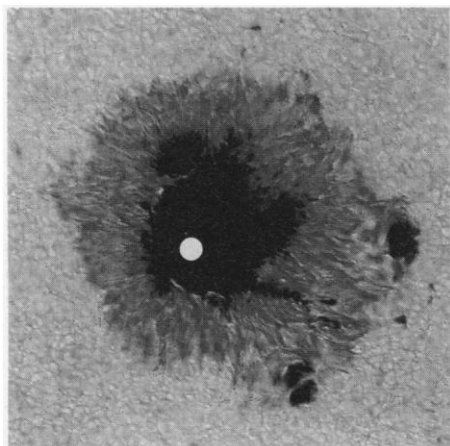


**Fig. 1.** A portion of the 26 July 1991 solar disk photographed in white light, which shows the 6000 K granulation field and a mature, much colder sunspot. In this reproduction, the sunspot umbra appears uniformly dark but has, in reality, brightness structure. The 7-arc sec white dot, representing the input aperture to the Fourier transform spectrometer, has been positioned in the darkest, coolest, umbral "void" (26) where the temperature falls to about 3500 K and the water molecule can form and exist.

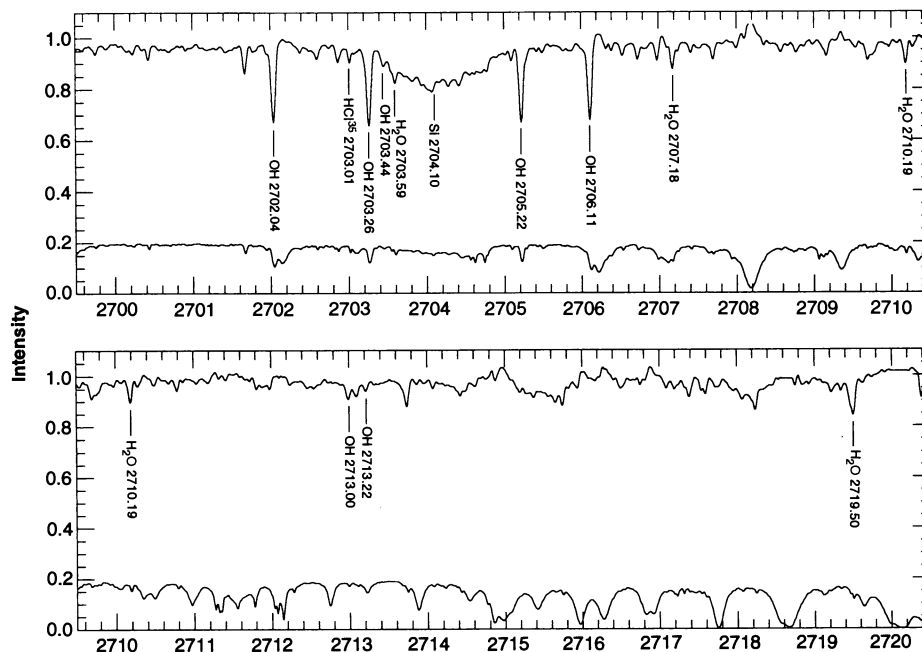


**Fig. 2.** A portion of the sunspot spectrum in the 3.7- $\mu\text{m}$  region (11). The lower trace in both panels is the observed spectrum recorded at an air mass of 2.3, and the upper trace is the spectrum corrected for atmospheric absorption by extrapolation to zero air mass. The two panels form a continuous spectrum.

two corrected umbral spectra. The upper trace in Fig. 3B is a somewhat warmer umbral spectrum recorded on 7 April 1981 and presented only for comparison purposes.

The identity of the dense molecular absorption was not obvious. Pure rotational lines of OH (9) and HF (14) can be found as well as the strong  $\Delta v = 1$  vibra-

tional bands of SiO (20, 21), but the remaining lines form no regular pattern and can have a density approaching 50 lines per reciprocal centimeter. It seemed likely that these lines are due to water, but the reported energy levels (15–18) were completely inadequate to confirm this. Therefore, new laboratory emission spectra of hot water were recorded at the University of Waterloo.

These new spectra were recorded at a resolution of  $0.01 \text{ cm}^{-1}$  in the regions from  $350$  to  $1000 \text{ cm}^{-1}$  and  $800$  to  $2900 \text{ cm}^{-1}$ . A flow of water vapor at a pressure of 15 torr was maintained in a mullite ( $3\text{Al}_2\text{O}_3 \cdot 2\text{SiO}_2$ ) tube furnace at  $1550^\circ\text{C}$ . A KBr beam splitter and a Si:B detector with a cold filter were used for the region from  $350$  to  $1000 \text{ cm}^{-1}$ , and a HgCdTe detector and an uncooled filter were used for the region from  $800$  to  $2900 \text{ cm}^{-1}$ . The observed line density in the region from  $700$  to  $900 \text{ cm}^{-1}$  is about 14 lines per reciprocal centimeter. This line density is still less than that observed in the umbra because the water in the laboratory is cooler.

A temperature of  $3200 \text{ K}$  for the umbra was derived from the  $\Delta v = 1$  SiO vibration-rotation lines. For a sunspot, this is a relatively low temperature (7) and is the reason why the molecular lines are so deep and prominent (Fig. 3). A temperature of  $3700 \text{ K}$  (20) was derived from the  $\Delta v = 1$  SiO lines by Glenar *et al.* (20) for the umbra that they observed.

In spite of the difference in temperature between the water in the laboratory spectrum ( $1820 \text{ K}$ ) and the water in the umbral spectrum ( $3200 \text{ K}$ ), most of the strong lines in the latter have corresponding laboratory features (Fig. 4). We conclude that the remarkably dense lines in the sunspot spectrum are due mainly to water. Moreover, most of the weaker unmarked lines in this spectrum are probably also due to water.

The column densities of water in the sunspot umbrae are difficult to estimate because the transition strengths of the highly excited rotational transitions are not reliably predicted. However, our preliminary estimate for the umbral spectrum of 26 July 1991, based on calculations (2) for a few clean lines near  $4000 \text{ cm}^{-1}$  and  $5700 \text{ cm}^{-1}$ , is  $2 \times 10^{19}$  molecules per square centimeter.

The water lines in the  $10\text{-}\mu\text{m}$  sunspot spectrum (Fig. 3) represent pure rotational transitions in the ground vibrational level and in various excited vibrational levels. No more than 20% of the lines in the new laboratory spectra can be assigned quantum numbers on the basis of the currently known energy levels. Water is a very asymmetric top with such large rotational constants that the Watson Hamiltonian normally used to represent the energy levels is divergent (22).

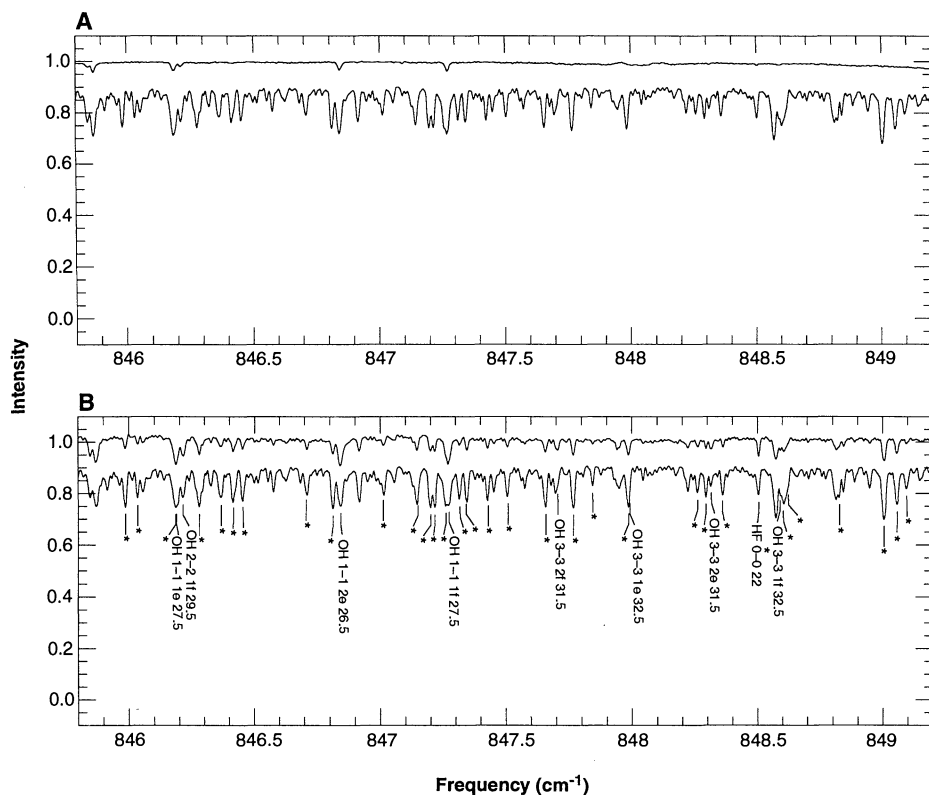


**Fig. 3.** A portion of the sunspot spectrum in the  $12\text{-}\mu\text{m}$  region. (A) The lower trace is the spectrum of the sunspot umbra and the upper trace is the spectrum of the penumbra, which serves as a reference spectrum to correct for atmospheric absorption. (B) The spectra of two different sunspots, corrected for atmospheric absorption [\* indicates a peak due to  $\text{H}_2\text{O}$ ]. The lower trace is the sunspot spectrum recorded on 4 March 1982, and the upper trace is the spectrum of another sunspot recorded on 7 April 1981. The umbral spectrum of 4 March 1982 has particularly strong molecular lines.

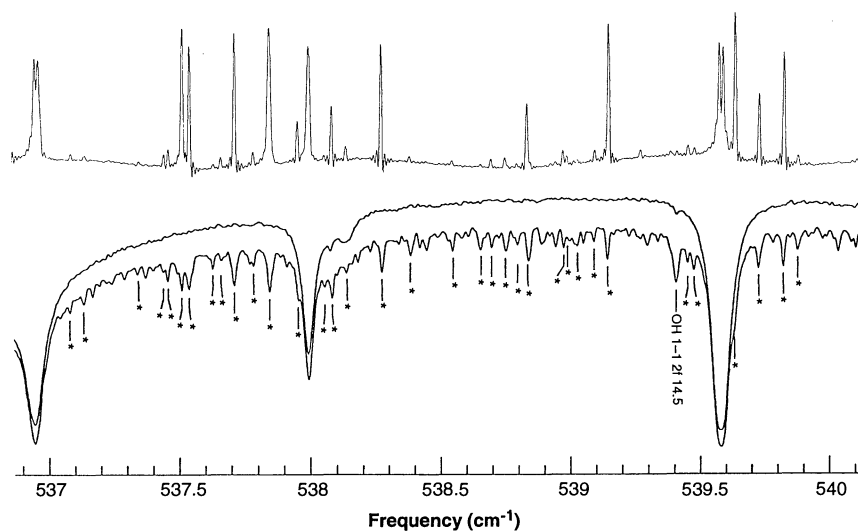


**Fig. 4.** A comparison between the laboratory emission spectrum (top trace) of hot water, the spectrum of a sunspot penumbra (middle trace), and a sunspot umbra (lower trace) [water peaks are indicated by (\*)]. The water features at  $537 \text{ cm}^{-1}$  and  $539.6 \text{ cm}^{-1}$  show self-absorption in the laboratory emission spectrum and correspond to telluric water features in the lower two traces.

This means that the necessary extrapolation of the known lower rotational  $J$  transitions to the unknown higher  $J$  transitions will fail with the traditional perturbation Hamiltonian. Some progress can be made if the divergent series is resumed with the use of Padé approximants (22) and other more sophisticated schemes (23). The assignment of the hot water vapor spectrum is therefore a difficult task (24). The water spectrum is of fundamental importance and presents such a theoretical challenge that new techniques (18, 25) for the calculation of spectra are often tested with it.

## REFERENCES AND NOTES

1. J. Liebert, in *Molecules in the Stellar Environment*, U. G. Jorgensen, Ed. (Springer-Verlag, Berlin, 1994), figure 1, p. 62; F. Allard, P. H. Hauschildt, S. Miller, J. Tennyson, *Astrophys. J.* **426**, L39 (1994).
2. K. H. Hinkle and T. G. Barnes, *Astrophys. J.* **227**, 923 (1979).
3. H. Spinrad and R. F. Wing, *Annu. Rev. Astron. Astrophys.* **7**, 249 (1969).
4. T. Tsuji and K. Ohnaka, in *Elementary Processes in Dense Plasmas*, S. Ichimaru and S. Ogata, Eds. (Adison-Wesley, Reading, MA, in press).
5. A. C. Cheung *et al.*, *Nature* **221**, 626 (1969).
6. J. C. Pearson, T. Anderson, E. Herbst, F. C. Delucia, P. Helminger, *Astrophys. J.* **379**, L41 (1991); T. Amano and F. Scappini, *Chem. Phys. Lett.* **182**, 93 (1991), and references therein.
7. R. J. Bray and R. E. Loughead, *Sunspots* (Dover, New York, 1979), p. 107.
8. K. Sinha, *Proc. Astron. Soc. Aust.* **9**, 32 (1991).
9. M. Geller, *A High-Resolution Atlas of the Infrared Spectrum of the Sun and the Earth Atmosphere from Space*, volume III, *Key to Identification of Solar Features* (NASA Ref. Publ. 1224, National Aeronautics and Space Administration, Washington, DC, 1992).
10. D. N. B. Hall, thesis, Harvard University (1970).
11. L. Wallace and W. Livingston, *An Atlas of a Dark Sunspot Umbra Spectrum from 1970 to 8640  $\text{cm}^{-1}$  (1.16 to 5.1  $\mu\text{m}$ )* (Natl. Solar Observ. Tech. Rep. 92-001, National Optical Astronomy Observatories, Tucson, AZ, 1992).
12. S. G. Kleinman and D. N. B. Hall, *Astrophys. J. Suppl. Ser.* **62**, 501 (1986).
13. D. N. B. Hall and R. W. Noyes, *Astrophys. J.* **175**, L95 (1972).
14. R. B. LeBlanc, J. B. White, P. F. Bernath, *J. Mol. Spectrosc.* **164**, 574 (1994).
15. J. M. Flaud, C. Camy-Peyret, J. P. Maillard, *Mol. Phys.* **32**, 499 (1976).
16. C. Camy-Peyret *et al.*, *ibid.* **33**, 1641 (1977).
17. R. A. Toth, *Appl. Opt.* **33**, 4851 (1994), and references therein.
18. O. L. Polyansky, P. Jensen, J. Tennyson, *J. Chem. Phys.* **101**, 7651 (1994), and references therein.
19. L. Wallace, W. Livingston, P. Bernath, *An Atlas of the Sunspot Spectrum from 470 to 1233  $\text{cm}^{-1}$  (8.1 to 21  $\mu\text{m}$ ) and the Photospheric Spectrum from 460 to 630  $\text{cm}^{-1}$  (16 to 22  $\mu\text{m}$ )* (Natl. Solar Observ. Tech. Rep. 1994-01, National Optical Astronomy Observatories, Tucson, AZ, 1994).
20. D. A. Glenar, A. R. Hill, D. E. Jennings, J. W. Brault, *J. Mol. Spectrosc.* **111**, 403 (1985).
21. J. M. Campbell, D. Klapstein, M. Dulick, P. F. Bernath, L. Wallace, in preparation.
22. O. L. Polyansky, *J. Mol. Spectrosc.* **112**, 79 (1985).
23. V. G. Tyuterev, *ibid.* **151**, 97 (1992).
24. O. L. Polyansky, J. Busler, B. Guo, K. Zhang, P. Bernath, in preparation.
25. U. G. Jorgensen and P. Jensen, *J. Mol. Spectrosc.* **161**, 219 (1993).
26. W. Livingston, *Nature* **350**, 45 (1991).
27. The National Optical Astronomy Observatories are operated by the Association of Universities for Research in Astronomy under cooperative agreement

with the National Science Foundation. We thank T. Tsuji for a copy of (4) in advance of publication. This work was supported by the Natural Sciences and Engineering Research Council of Canada. This work was supported in part by the Petroleum Re-

search Fund. Some support was also provided by the National Aeronautics and Space Administration Laboratory Astrophysics Program.

3 February 1995; accepted 17 March 1995

# The "Wake-Sleep" Algorithm for Unsupervised Neural Networks

Geoffrey E. Hinton,\* Peter Dayan, Brendan J. Frey, Radford M. Neal

An unsupervised learning algorithm for a multilayer network of stochastic neurons is described. Bottom-up "recognition" connections convert the input into representations in successive hidden layers, and top-down "generative" connections reconstruct the representation in one layer from the representation in the layer above. In the "wake" phase, neurons are driven by recognition connections, and generative connections are adapted to increase the probability that they would reconstruct the correct activity vector in the layer below. In the "sleep" phase, neurons are driven by generative connections, and recognition connections are adapted to increase the probability that they would produce the correct activity vector in the layer above.

Supervised learning algorithms for multilayer neural networks face two problems: They require a teacher to specify the desired output of the network, and they require some method of communicating error information to all of the connections. The wake-sleep algorithm avoids both of these problems. When there is no external teaching signal to be matched, some other goal is required to force the hidden units to extract underlying structure. In the wake-sleep algorithm, the goal is to learn representations that are economical to describe but allow the input to be reconstructed accurately. We can quantify this goal by imagining a communication game in which each vector of raw sensory inputs is communicated to a receiver by first sending its hidden representation and then sending the difference between the input vector and its top-down reconstruction from the hidden representation. The aim of learning is to minimize the "description length," which is the total number of bits that would be required to communicate the input vectors in this way (1). No communication actually takes place, but minimizing the description length that would be required forces the network to learn economical representations that capture the underlying regularities in the data (2).

The neural network has two quite different sets of connections. The bottom-up "recognition" connections are used to convert the input vector into a representation in one or more layers of hidden units. The

top-down "generative" connections are then used to reconstruct an approximation of the input vector from its underlying representation. The training algorithm for these two sets of connections can be used with many different types of stochastic neurons, but for simplicity, we use only stochastic binary units that have states of 1 or 0. The state of unit  $v$  is  $s_v$ , and the probability that it is on is

$$\text{Prob}(s_v = 1) = \frac{1}{1 + \exp(-b_v - \sum_u s_u w_{uv})} \quad (1)$$

where  $b_v$  is the bias of the unit and  $w_{uv}$  is the weight on a connection from unit  $u$ . Sometimes the units are driven by the generative weights, and at other times they are driven by the recognition weights, but the same equation is used in both cases (Fig. 1).

In the "wake" phase, the units are driven bottom-up with the recognition weights; this produces a representation of the input vector in the first hidden layer, a representation of this representation in the second hidden layer, and so on. All of these layers of representation combined are called the "total representation" of the input, and the binary state of each hidden unit  $j$  in the total representation  $\alpha$  is  $s_j^\alpha$ . This total representation could be used to communicate the input vector  $d$  to a receiver. According to Shannon's coding theorem, it requires  $-\log r$  bits to communicate an event that has probability  $r$  under a distribution agreed upon by the sender and receiver. We assume that the receiver knows the top-down generative weights (3), so that these can be used to create the agreed probability distributions required for communication. First, the activ-

Department of Computer Science, University of Toronto, 6 King's College Road, Toronto, M5S 1A4, Ontario, Canada.

\*To whom correspondence should be addressed.